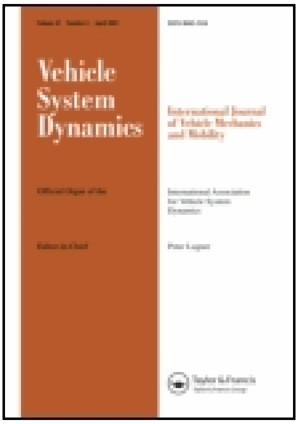

Vehicle System Dynamics: International Journal of Vehicle Mechanics and Mobility

Publication details, including instructions for authors and subscription information:
http://www.tandfonline.com/loi/nvsd20

The stability mechanism and its application to heavy-haul couplers with arc surface contact

Yuan Yao [a], Xiao-xia Zhang [b], Hong-jun Zhang [a] & Shi-hui Luo [a]

[a] State Key Laboratory of Traction Power, Southwest Jiaotong University, 610031, Chengdu, People's Republic of China

[b] College of Nuclear Technology and Automation Engineering, Chengdu University of Technology, 610059, Chengdu, People's Republic of China

Published online: 31 May 2013.

To cite this article: Yuan Yao, Xiao-xia Zhang, Hong-jun Zhang & Shi-hui Luo (2013) The stability mechanism and its application to heavy-haul couplers with arc surface contact, Vehicle System Dynamics: International Journal of Vehicle Mechanics and Mobility, 51:9, 1324-1341, DOI: 10.1080/00423114.2013.801500

To link to this article: http://dx.doi.org/10.1080/00423114.2013.801500

Vehicle System Dynamics, 2013
Vol. 51, No. 9, 1324–1341, http://dx.doi.org/10.1080/00423114.2013.801500

The stability mechanism and its application to heavy-haul couplers with arc surface contact

Yuan Yao[a]*, Xiao-xia Zhang[b], Hong-jun Zhang[a] and Shi-hui Luo[a]

[a]*State Key Laboratory of Traction Power, Southwest Jiaotong University, 610031 Chengdu, People's Republic of China;* [b]*College of Nuclear Technology and Automation Engineering, Chengdu University of Technology, 610059 Chengdu, People's Republic of China*

(*Received 24 January 2013; final version received 28 April 2013*)

To investigate the stability mechanism of a type of heavy-haul coupler with arc surface contact, the force states of coupler were analysed at different yaw angles according to the friction circle theory and the structural characteristics of this coupler were summarised. A multi-body dynamics model with four heavy-haul locomotives and three detailed couplers was established to simulate the process of emergency braking. In addition, the coupler yaw instability was tested in order to investigate the effect of relevant parameters on the coupler stability. The results show that this coupler exhibits the self-stabilisation and less lateral force at a small yaw angle. The yaw angle of force line is less than the actual coupler yaw angle which reduces the lateral force and the critical instability. An increase in the friction coefficient of the arc contact surfaces can improve the stability of couplers. The friction coefficient needs to be increased with the increase in the maximum coupler longitudinal compressive force. The stability of couplers is significantly enhanced by increasing the secondary suspension stiffness and reducing the clearance of the lateral stopper of the locomotives. When the maximum coupler compressive force reaches 2500 kN, the required friction coefficient reduces from 0.6 to 0.35, which notably lowers the derailment risk caused by the coupler. The critical instability angle of the coupler mainly depends on the arc contact friction coefficient. When the friction coefficient is 0.3, the critical instability angle was 4–4.5°. The simulation results are consistent with the locomotive line tests. These studies establish meaningful improvements for the stability of couplers and match the heavy-haul locomotive with its suspension parameters.

Keywords: heavy-haul coupler; coupler stability; friction circle; locomotive; derailment

1. Introduction

A large longitudinal compression force makes the coupler yaw unstable when the heavy-haul train is braking. The larger yaw angle of coupler will produce a greater lateral force which may lead to the locomotive's derailment. As one of the key equipment items of the railway heavy-haul transport, the yaw stability requirements of the heavy-haul coupler are required to increase as train tonnage and speed increase. The derailment caused by coupler occurs occasionally when the train is in emergency breaking,[1–5] which leads to a strong need of better understanding from the production, operations departments and academic institutions.

*Corresponding author. Email: yyuan8848@163.com
This article was originally published with errors. This version has been amended. Please see Corrigendum (http://dx.doi.org/10.1080/00423114.2013.818843).

Several researchers previously investigated the longitudinal dynamics of a long train, and discussed the effects of buffer parameters on longitudinal impact forces of the train.[6,7] Cole *et al.* [8], Simson and Cole [9] and Cole and Sun [10] conducted many studies on the derailment issues involving heavy-haul trains, such as longitudinal train dynamics, the modelling of the wagon connection model, comfort, train management and driving practices. A comprehensive nonlinear model was developed [11] to study severe braking conditions to minimise the tendency of train derailment. However, these studies did not consider the coupler stability problem under longitudinal compressive forces applied on the coupler.[12,13] The current understanding of the heavy-haul train coupler stability and its effect on derailment are still rudimentary and need to be studied further.

The couplers of heavy-haul locomotive can be divided into two types according to the structure in China currently. The first sets an elastic stopper which can prevent a larger yaw angle to provide the lateral stability of the coupler. Ma *et al.* [2] studied the effects of this coupler and buffer systems on the dynamic performance of heavy-haul locomotives to better understand possible derailment issues during braking. The second has an arc contact surface in the end of the coupler. Wu et al.[14] used rotate joint to simulate the yoke key of this coupler, and postulated that the friction torque supplied by two end contact surfaces will balance the yaw moment caused by the coupler yaw angle to stabilize the coupler. Practical application has shown that a solution to the locomotive derailment caused by the first type of the coupler is reducing the yaw angle gap of the elastic stopper. For the second type of the coupler, the yaw angle is not large and reducing the gap of the yaw stopper to improve the stability is not effective. Through the kinematic and static force analysis, a solution for the instability of the second type of the coupler is proposed according to the theory of friction circle. These studies have theoretical and practical engineering value to improve the bearing capacity of this coupler.

2. The structural characteristics of the coupler with arc surfaces contact

2.1. *The coupler structure*

The diesel-electric locomotive coupler used in China is shown in Figure 1. Note that both ends and the followers have an arced surface which is used to transfer the longitudinal compressive force. The coupler and the coupler yoke are connected by a yoke key. When the coupler is pulled, the coupler pulls the yoke key and moves the coupler yoke, thus compressing the

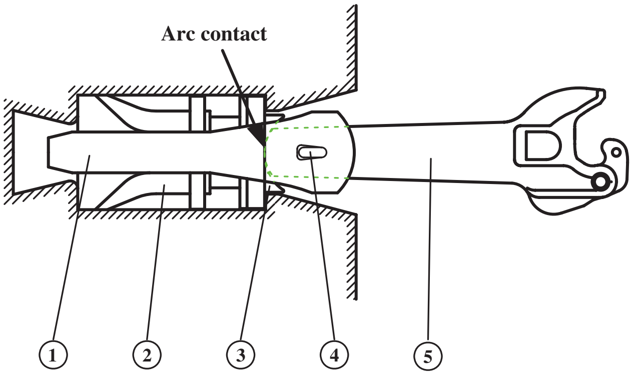

Figure 1. The structure diesel-electric locomotive coupler with arc contact.

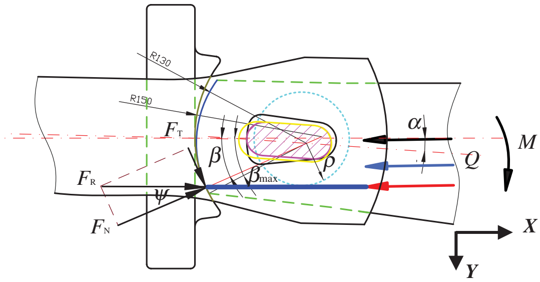

Figure 2. The contact analysis of the end arc surfaces.

rubber buffer to provide the traction stiffness and damping. When the coupler is compressed, the yoke key cannot transfer the longitudinal compressive force and instead, it is transferred by the arc surface contact to compress the rubber buffer. The arc radii of the follower and the end of coupler are 150 and 130 mm, respectively. The unequal arc radii make the two arc surfaces rolling instead of sliding which is the key mechanism for this coupler.

2.2. *The contact analysis of arc surfaces*

The contact analysis of the end arc surfaces is shown in Figure 2. The contact between the follower and the coupler end is a line of contact because the radii are different. When the coupler rotates and the yaw angle is α, the position of the contact point moves along the arc because of the tangential friction force. The angle between the centre line of the follower and the contact point (called the contact angle) is β. Assuming that the friction of the contact surfaces is not saturated, the two arc contact surfaces are pure rolling. The angles of α and β satisfy the following relationship:

$$\beta = \frac{r}{R - r}\alpha, \tag{1}$$

where R and r are the respective radius of the follower and the end of coupler.

During braking, the coupler experiences the longitudinal compressive force, Q, and the yaw moment, M, when the coupler has a certain yaw angle. The M is equivalent to the Q translated in the lateral direction, a distance of L, where $L = M/Q$. The moved force line is the actual transfer force line and it passes through the contact point. According to the friction circle theory, a friction circle with a radius ρ is drawn in the circle centre of the arc surface in the coupler end and is shown in Figure 2. The ρ and friction coefficient μ of arc contact have the following relationship:

$$\rho = r \sin(\tan^{-1} \mu). \tag{2}$$

When the L is smaller than ρ, the friction does not reach saturation and the contact is in the pure rolling state. When the L equals ρ, the contact is in the critical state and the force line is tangent to the friction circle. When the L is larger than ρ, the two arc surfaces slide. When the relative lateral displacement of the two car bodies increases from 0, the angle α and β increase at the beginning of the rolling contact process. When α reaches a certain value, the rolling friction reaches its limitation and the adhesion state between the two contact surfaces changes from stick to slip in the opposite direction. At this point, β has an inverse relationship with α. The coupler experiences the tangent friction and the normal support force at the contact point. The resultant force will deflect the direction of the external force once the friction reaches saturation which will make the coupler change into instability easily.

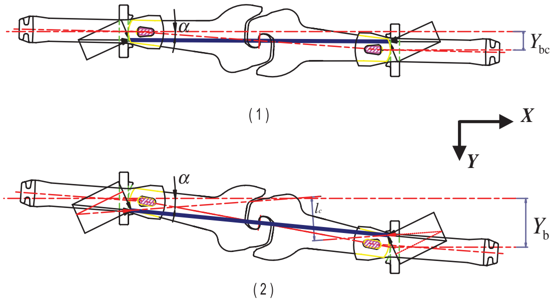

Figure 3. The two states of the force line.

The maximum lateral displacement of the contact point depends on the actual width of the coupler end. The maximum contact angle β equals 28° in the Chinese heavy-haul coupler. At this point, the coupler maximum yaw angle α is 4.3° in the condition of pure rolling, where the requirement of the friction coefficient μ is at least 0.53.

2.3. *The stability mechanism of the coupler*

The structure is symmetric when the two diesel-electric locomotive couplers are connected. The force line is located in the inner common tangent line of the two friction circles at the two ends of the coupler in the critical roll-slip state, where the lateral relative displacement, Y_b, between the two car bodies connected by a coupler is defined as the car body critical lateral relative displacement, Y_{bc}, and the corresponding coupler yaw angle is defined as the coupler critical yaw angle α_c. The Y_{bc} and α_c are dependent on the friction coefficient μ. When α is smaller than α_c, the direction of the force line (the connection line between the two arc contact points) is consistent with the resultant force at the contact point.

During braking, the couplers experience longitudinal compressive force mainly. The direction of the force line parallels with the track as state 1 in Figure 3 at a small yaw angle of the coupler, where the coupler lateral forces do not occur. When the force line deflects the track, the coupler's lateral force will appear as state 2 in Figure 3 where the yaw angle of force line is less than the coupler's actual yaw angle. If the friction coefficient of the arc contact is large enough, the resultant force at the arc contact point moves along the direction of the force line, and the arc surfaces cannot slide, while the force line deflects the track direction that will produce the coupler lateral force. The coupler's lateral forces move the car bodies, and it is balanced by the secondary suspension of locomotive. These lateral forces are transferred to the bogie and increase the wheelset lateral forces. Once the coupler's lateral forces cannot be balanced by the wheelset lateral forces, the locomotive will derail.

The critical instability angle α_{cs} depends on the coupler's longitudinal compressive force and the parameters of the locomotive and coupler. In order to improve the coupler stability, the secondary suspension lateral stiffness of the locomotive and the arc surface friction coefficient of the couplers should be increased as well as the secondary lateral stopper clearance should be reduced.

2.4. *The geometric analysis of the coupler and the force line*

Figure 4 shows the geometric relationships of the coupler and the force line. Ignoring the car body yaw angle η, the geometric relationships between the angle θ of the force line to the

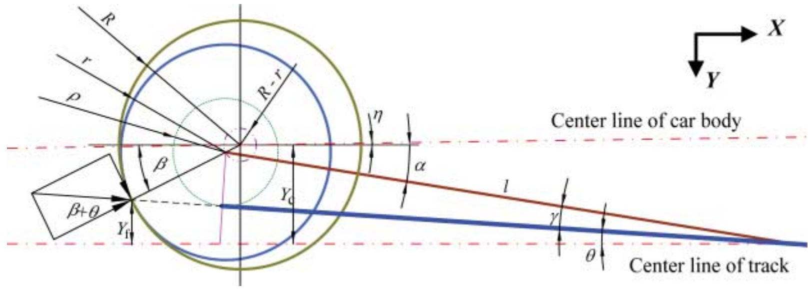

Figure 4. The geometric analysis of the coupler and the force line.

Table 1. The parameters of couple in the critical roll-slip state.

μ	ρ (mm)	$2Y_{bc}$ (mm)	γ_{max} (°)
0.2	25.5	58.83	2.05
0.3	37.36	86.2	3.01
0.4	48.28	111.4	3.89
0.5	58.14	134.2	4.68

track centreline, and the angle γ of the force line to the coupler centreline are as follows:

$$\gamma = \sin^{-1}\left(\frac{\rho}{l}\right), \tag{3}$$

$$\beta + \theta = \tan^{-1}\mu, \tag{4}$$

$$\alpha = \gamma + \theta, \tag{5}$$

where l is half of the coupler length, which was 712 mm for these studies.

When the matching of the two radii is optimal, the car body critical lateral displacement Y_{bc} is

$$Y_{bc} = R\sin(\tan^{-1}\mu). \tag{6}$$

The corresponding parameters of the coupler in the critical roll-slip state are given in Table 1. These are related to the friction coefficient μ and the radius R and r, and the length of coupler $2l$.

When $Y_b \leq Y_{bc}$, the force line moves along the track direction, as states (1) and (2) in Figure 5.

When $Y_b > Y_{bc}$, the force line deflects the track direction as state (3) in Figure 5. There is a lateral force that appears between the two car bodies caused by the coupler.

The contact points of the arc surfaces are located at the intersection of the force line and the arc surfaces. With the increase in the coupler yaw angle, the contact point moves along the arc and the contact angle β increases. When the contact surfaces begin to slide in the opposite direction, β reaches its maximum. The lateral movements of the contact points at the both ends of coupler help to reduce the coupler's lateral forces.

2.5. *The arc radii optimisation*

According to the coupler geometry analysis, the arc radii determine the lateral positions of the contact points even for the same yaw angle of the coupler. Decreasing the follower radius R and increasing the end radius r within a certain range are conducive to increasing the lateral position Y_c and the contact angle β. However, the larger β makes the contact surfaces slide

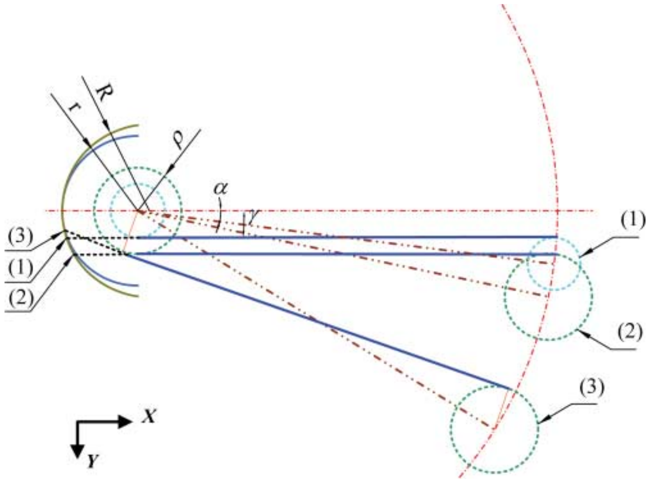

Figure 5. The three typical states of the force line.

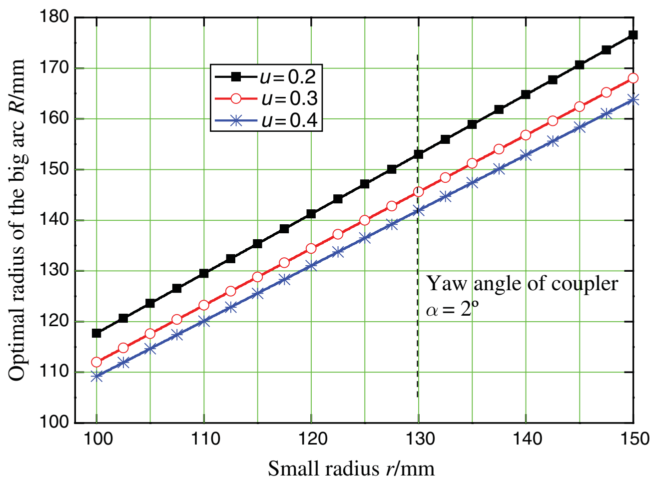

Figure 6. The optimal relationship of arc radii at a yaw angle of 2°.

easier, thus requiring a higher friction coefficient. If the force line is exactly parallel to the track direction when the arc surfaces are in the critical roll-slide state, the lateral position of the contact points will be larger and the coupler will be more stable. The optimal relationship of the two arc radii is shown in Figures 6 and 7 at different yaw angles of couple. It is obtained by a careful optimisation that the R is 20 mm larger than r.

2.6. *Summary*

The coupler with arc surface contact transfers the longitudinal compressive forces using the force line which is the connection of the two contact points in both ends. This type of coupler has the following characteristics:

(1) At a small yaw angle, the force line parallels the track direction and the lateral force of the coupler can be ignored.

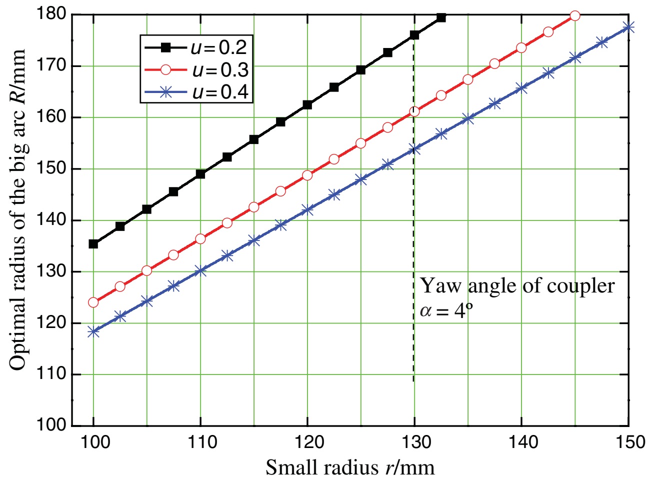

Figure 7. The optimal relationship of arc radii at a yaw angle of 4°.

(2) The yaw angle of the force line is less than the actual yaw angle of the coupler, which can reduce the lateral coupler forces.
(3) The rolling friction of the arc surfaces reduces the yaw resistance of coupler, which can decrease the lateral coupling effects between the car bodies connected by a coupler.

In conclusion, this type of coupler exhibits self-stabilisation and a smaller lateral force at a small yaw angle when it is compressed. At a larger yaw angle, the lateral coupler forces are balanced by the secondary suspension of the locomotive. If the yaw moment is greater than the balance moment, the coupler will overturn and cause locomotive derailment. Increasing the secondary suspension stiffness and the coupler friction coefficient as well as reducing the lateral stopper clearance of the secondary suspension of locomotives are effective measures to improve the bearing capacity of this type of coupler.

3. Multi-locomotive dynamic simulation model

In order to verify the theoretical analysis and to find the relationship between the coupler's bearing capacity and the secondary suspension parameters of locomotive accurately, the multi-body dynamics software, SIMPACK, was used to build the locomotive and the detailed coupler model. The simple train model which is composed of four locomotives can simulate the processes of the emergency braking and the coupler overturn with appropriate boundary conditions. The main impact factors of the coupler's bearing capacity had been analysed.

3.1. *The locomotive dynamic model*

This locomotive model was established according to an actual heavy-haul locomotive in China, as given in Table 2. Several derailment accidents caused by emergency braking had happened in a straight line for this locomotive. Two improvements are proposed in this paper to solve the locomotive's derailment. The three parameter set-ups of the locomotives are given in Table 3. The model consists of four locomotives and three couplers as shown in Figure 8. The longitudinal forces, $F1$ and $F2$, are applied on the both ends of locomotives separately and

Table 2. The main parameters of locomotives.

Axle arrangement	Axle load (T)	Wheel base (m)	Bogie distance (m)	Coupler seats distance (m)
$2B_0$	25	2.6	10.6	17.652
Axle guidance stiffness(signal axlebox) ($\mathrm{kN\,mm^{-1}}$)			Secondary vertical suspension stiffness (one side in a bogie) ($\mathrm{kN\,mm^{-1}}$)	
Longitudinal 164.5	Lateral 5.95	vertical 2.123	1.07	

Table 3. The secondary lateral suspension parameters of locomotives.

Item	Stopper clearance (mm)	Stopper stiffness ($\mathrm{kN\,mm^{-1}}$)	Spring stiffness (one side in a bogie) ($\mathrm{kN\,mm^{-1}}$)
Origin	$20 + 40$	1.11	0.265
Improvement 1	$25 + 10$	2	0.42
Improvement 2	$25 + 10$	2	0.6

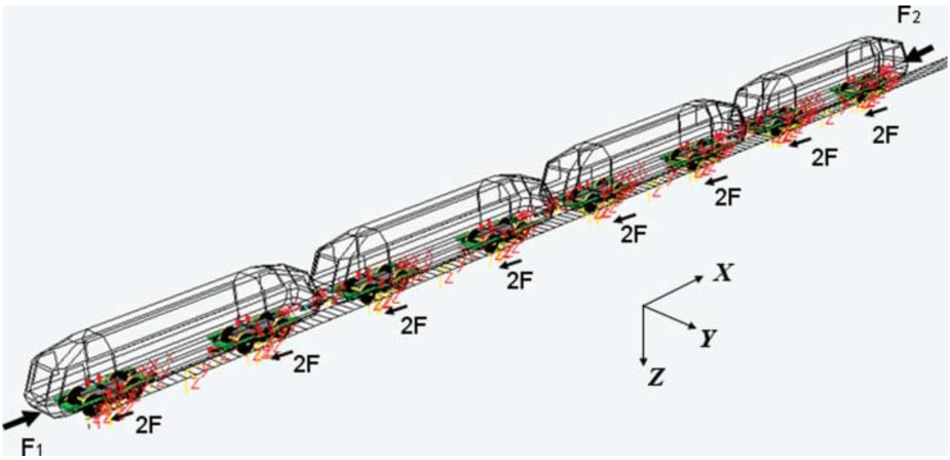

Figure 8. The simple train model composed of four locomotives and three couplers.

the braking torques are applied on each wheelset to simulate the longitudinal impulse caused by emergency braking. The middle two locomotives are taken as the focus of these studies.

3.2. *The coupler dynamic model*

The No. 18 contact force and the No. 100 nonlinear friction force element of SIMPACK are used to simulate the arc surfaces contact of the coupler. There are five rigid bodies in a coupler dynamic model as shown in Figure 9. The follower has the freedom to move longitudinally and to pitch, and the coupler has the freedom to move longitudinally, laterally and to yaw. The rubber buffer used in this coupler has a capacity greater than 100 kJ and its energy absorption ratio is greater than 80%. The upper and lower envelope curves are set by using No. 105 force element to simulate the buffer characteristics. The yaw stoppers of the coupler are set at both ends and the maximum yaw angle is 12°.

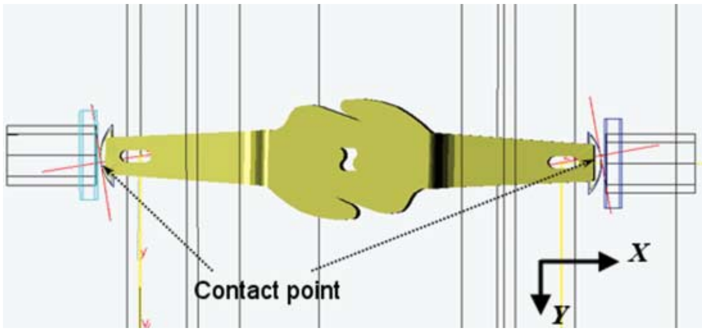

Figure 9. The coupler dynamic model.

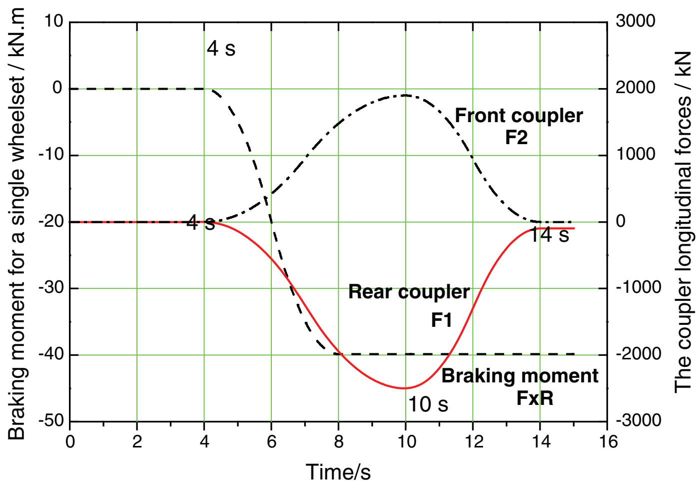

Figure 10. The boundary conditions and calculation conditions.

3.3. *The boundary conditions and calculation conditions*

To simulate the locomotives located in the middle of a 20,000 ton heavy-haul train in a straight line, the maximum coupler longitudinal impact force of 2500 kN and the initial speed before breaking of 80 km/h, and the braking force of 255 kN for a single locomotive are set as the boundary conditions. The track irregularity of AAR5 [15] is used to simulate the coupler stability. The simulation boundary conditions are shown in Figure 10. The time from the start of braking to the maximum coupler force is 6 s and the release time is 4 s.

4. The dynamic simulation of coupler

The static force analysis and the stability mechanism of the coupler in Section 2 are based on the assumption of static equilibrium. The coupler has a certain mass and inertia which result in the possibility that the force line may not be located in the ideal position in a timely manner in the dynamic process. Therefore, there is a certain lateral force in the case of a small yaw

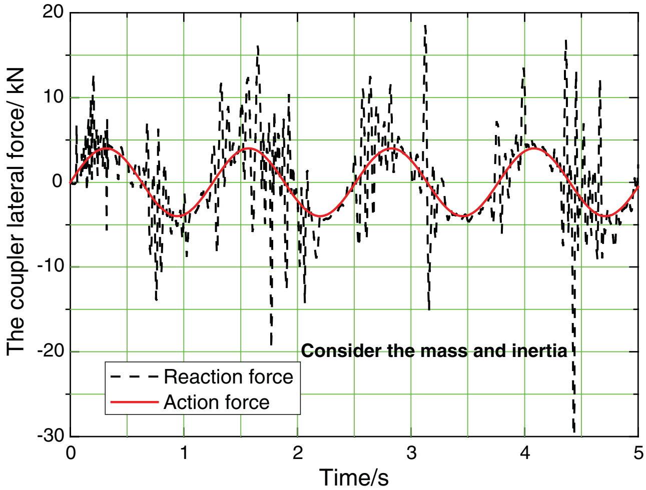

Figure 11. Simulation results considering the coupler mass and inertia of the coupler.

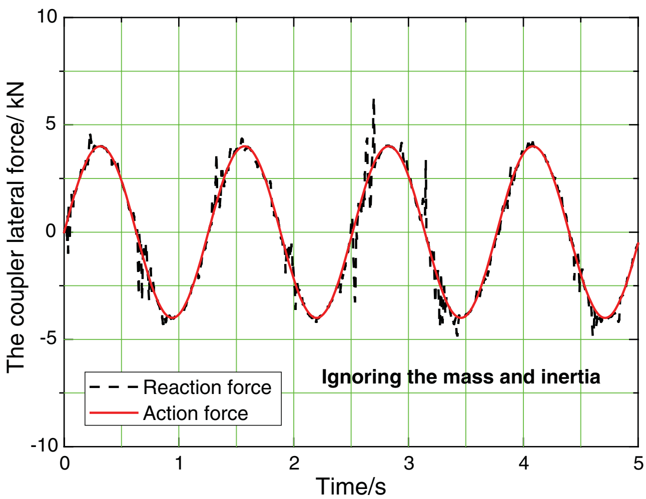

Figure 12. Simulation results ignoring the coupler mass and inertia of the coupler.

angle of the coupler caused by the non-ideal force line. The dynamic process of the coupler is simulated with the dynamic model shown in Figure 9.

One end of the coupler is fixed and to the other end is applied a lateral sinusoidal load as well as a large longitudinal compressive force. The arc surface friction coefficient is assumed large enough so that the coupler will not exhibit instability. The lateral force simulation results considering and not considering coupler mass and inertia are shown in Figures 11 and 12, respectively. When the coupler mass and inertia are considered, there are large 'burrs' included in the lateral reaction force of the fixed end (dotted line), in addition to the balance of applied lateral forces, which is the lateral component of the longitudinal coupler force generated by the non-ideal force line. When the coupler mass and inertia are ignored, the force line is located in the ideal position and the coupler's lateral force is consistent with the theoretical analysis. The greater the coupler inertia and yaw angular acceleration, the more the deflection angle between the force line and the ideal location which would influence the stability of the coupler.

5. The simulation results of the coupler stability

5.1. *The required minimum friction coefficient*

The required minimum friction coefficients for the coupler stability, which are shown in Figure 13, were determined through simulations based on the dynamics models and the operating conditions in Section 3. The required minimum friction coefficient increased with corresponding increases in the coupler's longitudinal force. When the maximum coupler force of 2500 kN was applied, the minimum friction coefficient of the original locomotive and the two improvements are 0.6, 0.4 and 0.35, respectively. By reducing the clearance of the secondary lateral stopper and increasing the secondary suspension lateral stiffness, the coupler stability of the locomotive has been significantly improved. The proposed modifications of increasing the secondary lateral suspension stiffness will affect the locomotive's lateral riding, the curves and switches passing capability. However, compared with the anti-derailment safety, it may be appropriate to reduce some of the non-safety performances. The simulation results in Figure 13 are for a new wheel tread. Wear of the wheel rim increases the wheel–rail clearance, which will increase the coupler yaw angle. Therefore, there is a need to ensure that the coupler friction coefficient and locomotive secondary lateral stiffness have a large safety margin.

Figure 14 shows the yaw angles of the coupler with different friction coefficients μ. As shown, the smaller the μ, the less stable the coupler is. The coupler instability will lead to instantaneous increase in the coupler yaw angle until the yaw stopper is contacted. The direction of the coupler overturning is random. If the actual friction coefficient is less than the minimum friction of the requirements in Figure 13, the coupler will yaw to the stopper which can cause a traffic safety accident. In Figure 14, the maximum yaw angle of the coupler is 3.36° when the friction coefficient is 0.4 and it is less than the angle $\gamma_{\max}$ in Table 1.

5.2. *The allowable maximum yaw angles according to the wheelset lateral forces*

In fact, the locomotive has been derailed due to the excessive wheel–rail lateral forces when the coupler is unstable. According to the biggest wheelset lateral force in BS EN14363, the

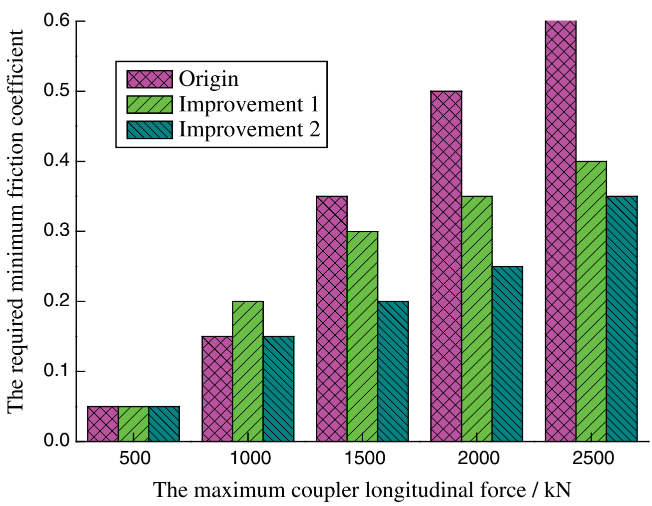

Figure 13. The required minimum friction coefficient for coupler stability.

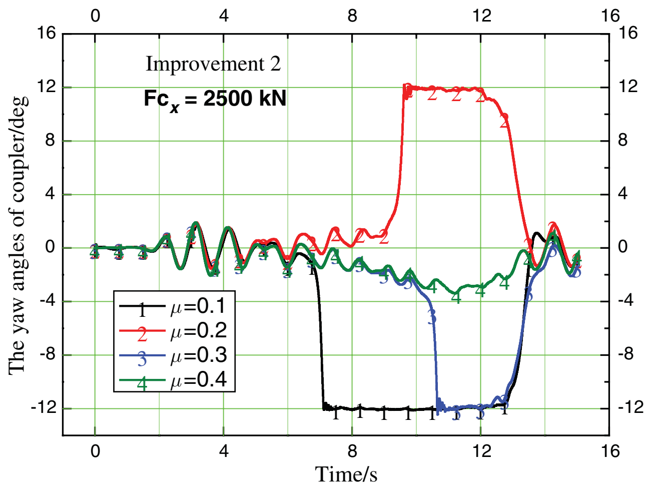

Figure 14. The yaw angle of coupler with different friction coefficients.

Table 4. The allowable maximum yaw angles when the wheelset lateral forces are not excessive.

		α_{max} (°)		
F_{xc} (kN)	θ_{max} (°)	$\mu = 0.2$	$\mu = 0.3$	$\mu = 0.4$
500	5.97	8.03	8.98	9.86
1000	2.99	5.05	6	6.88
1500	2	4.05	5.01	5.89
2000	1.5	3.55	4.51	5.39
2500	1.2	3.25	4.21	5.09

maximum permissible yaw angle of the force line can be calculated:

$$\theta_{max} \leq \tan^{-1}\left(\frac{L_b}{L_c F_{xc}}\left(10 + \frac{2Q_0}{3}\right)\right), \tag{7}$$

where L_b and L_c, are the longitudinal distance of the bogie centre and the coupler fixing seats at both ends of car body separately; F_{xc}, is the biggest coupler longitudinal force (kN); $2Q_0$ is the axle load of locomotive (kN). According to Formulae (2)–(5), the maximum permissible yaw angle of the coupler is

$$\alpha_{max} = \theta_{max} + \sin^{-1}\left(\frac{r}{l}\sin(\tan^{-1}\mu)\right). \tag{8}$$

The allowable maximum yaw angles of the force line and the coupler at the different coupler longitudinal forces and the different friction coefficient are given in Table 4. Normally, the coupler will become unstable before the yaw angle of the coupler reaches the value in Table 4. Therefore, the study was more concerned about the coupler critical instability angles in different conditions.

5.3. *The critical instability angle of the coupler*

In order to calculate the maximum stable yaw angles of the coupler at different friction coefficients of the arc contact surface and the different longitudinal compressive forces, the coupler's longitudinal force was increased gradually from 0. When the coupler force reaches a certain

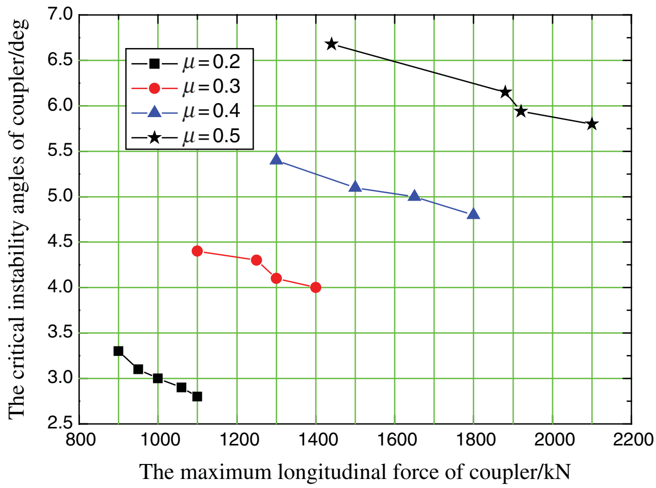

Figure 15. The coupler critical instability angles of the origin locomotive.

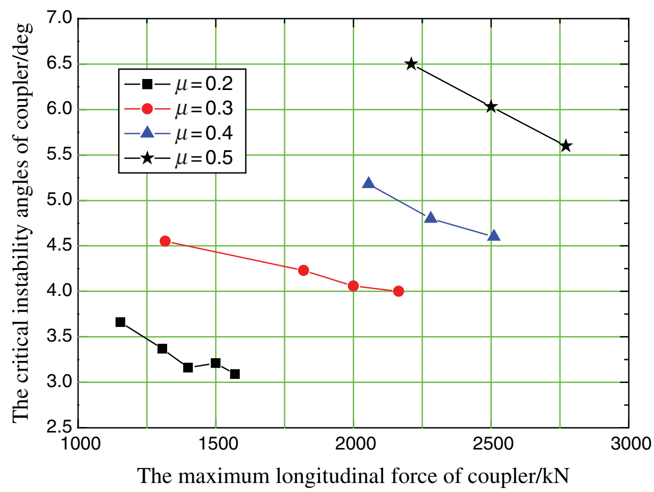

Figure 16. The coupler critical instability angles of the improvement 1 locomotive.

value, the coupler will become unstable. The corresponding yaw angle is the critical instability angle α_{cs} at this load. The calculated α_{cs} of the original and the two improved locomotives are shown in Figures 15–17. These figures show that the arc contact surface friction coefficient is the main factor affecting the bearing capacity of the coupler. Although the bearing capacity of the coupler is increased significantly by improving the secondary suspension, the critical instability angle α_{cs} has no significant influence. When μ is 0.3, the α_{cs} is between 4.0° and 4.5°.

6. The dynamic simulation and line tests of the locomotive and the coupler

6.1. *The running simulation in straight line*

There are several derailment accidents that occur with the original locomotive running in the straight line. The locomotives had been improved with improvement 2 by increasing the

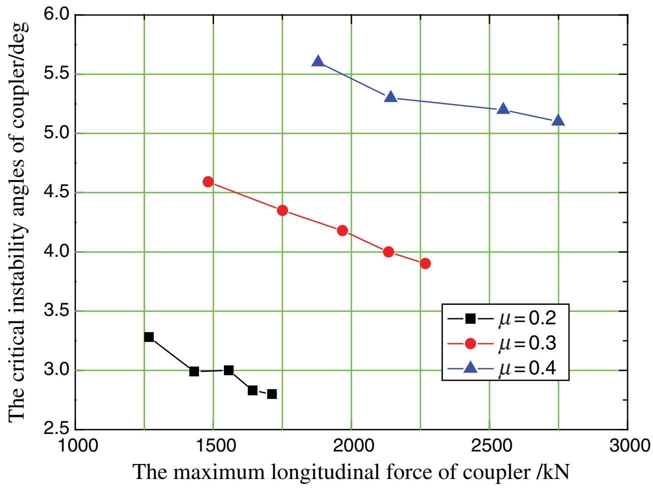

Figure 17. The coupler critical instability angles of the improvement 2 locomotive.

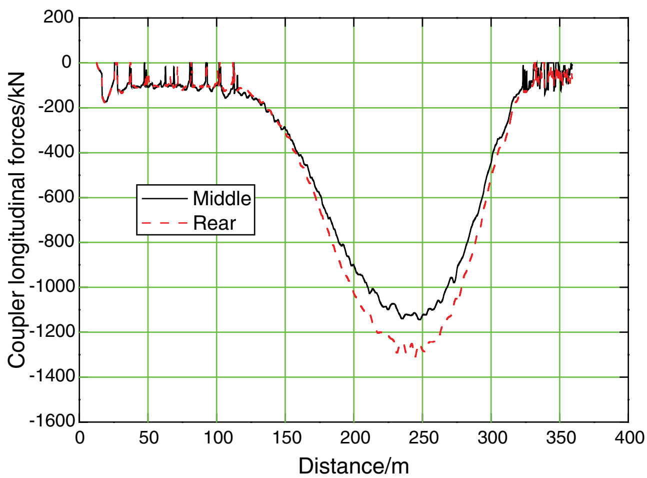

Figure 18. Simulated coupler longitudinal forces.

secondary lateral stiffness and reducing the gap of the secondary lateral stopper. The improved locomotives are simulated and tested in China's Daqin heavy-haul railway. The simulation dynamic models and boundary conditions are used in Section 3 and the middle two locomotives are the inspection objects.

In the simulation, the locomotive's initial speed was 80 km/h and the arc surfaces contact friction coefficient was 0.3. AAR4 and AAR5 class irregularities were used for the different track conditions. The maximum forces of the middle and rear couplers are 1150 and 1300 kN for the middle double locomotives according to the results of the line tests. The simulation coupler's longitudinal forces are shown in Figure 18, and the coupler's lateral forces at different track irregularities are shown in Figure 19. Figures 20 and 21 show the yaw angles of the coupler and the force line with the two irregularities. Under these calculation conditions, the coupler was stable. When the AAR4 class irregularity was used, the yaw angles of the coupler and the force line are larger because of a bigger lateral relative displacement of the car bodies, which

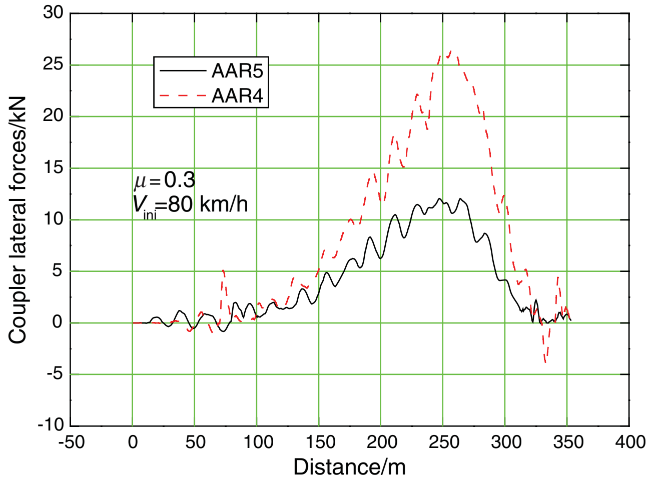

Figure 19. Simulated coupler lateral forces.

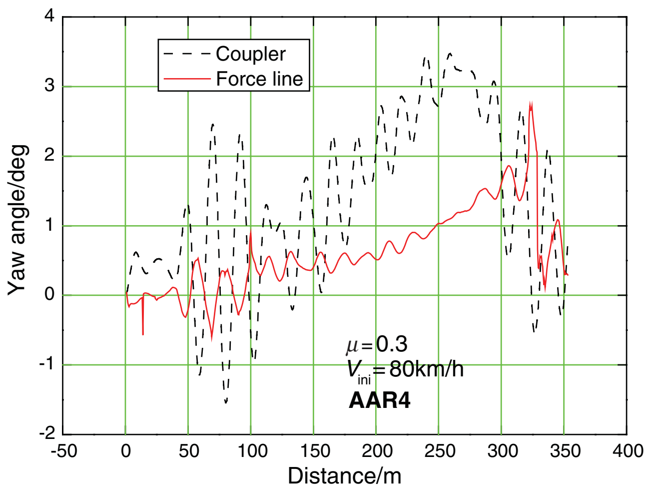

Figure 20. The yaw angles of coupler and line force in the AAR4 line.

results in a larger coupler lateral force. When the coupler suffers from a huge longitudinal compressive force, the dynamic amplitude of the yaw angle of the coupler is small.

At the AAR4 class track, the maximum yaw angle of the coupler reaches 3.4° and the maximum lateral relative displacement of the car bodies connected by a coupler is 84.45 mm, which is less than the car body critical lateral displacement of 86.20 mm in Table 1. That is, the yaw angle of the force line is ideally 0, but the force line deflects the ideal position which then produces a lateral force due to the inertia of the coupler. There is a certain phase difference between the angles of force line and the coupler in Figures 20 and 21. The larger the yaw angular velocity of the coupler, the more obvious deflection angles of the force line. This is inconsistent with the premise of the theoretical analysis in Section 2 because of the sliding between the arc contact surfaces. The force line yaw angle increases with increase in coupler yaw angle. After the brake releasing, the coupler is pulled instantaneously which can lead to larger fluctuations of the force line yaw angle because the contact points of arc surfaces slip due to the decrease in the contact preload.

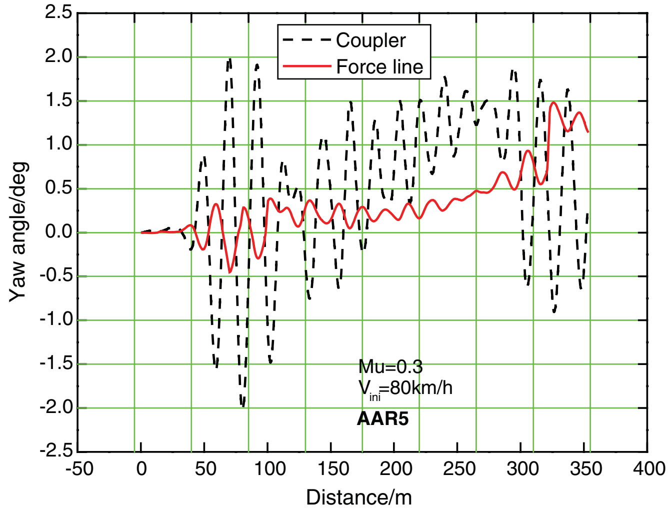

Figure 21. The yaw angles of coupler and line force in the AAR5 line.

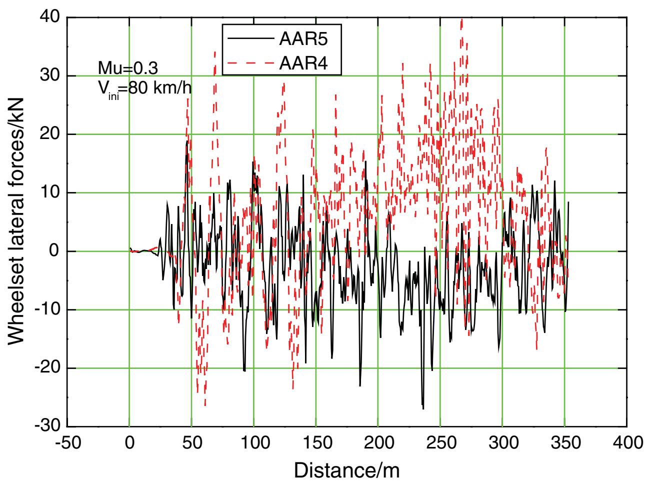

Figure 22. The wheelset lateral forces of the two class irregularities.

Figure 22 shows the simulation results of the wheelset lateral forces in a straight line. The maximum values are 27 and 40 kN at the two class irregularities, respectively, when the coupler longitudinal forces reach a maximum. As long as the coupler is stable, the wheelset lateral forces do not exceed the track's allowed values. Because the coupler's yaw direction is random, the maximum wheelset lateral force direction is random.

6.2. *The field tests*

The Datong–Qinhuangdao line is the first electrified heavy-haul railway for the coal transport in China, and now the traction tonnage reaches 20,000 ton. The test section is from Hudong to Chawu. The main three braking positions are located in the distance of K63, where there is a long down ramp, with air braking, while both K141–K181 and K275–K325 use electric and air braking. The braking tests were completed three times in the later two sections, respectively. Table 5 lists the test results of the locomotives in the middle train at China's Daqin heavy-haul

Table 5. The test results of the middle locomotive in China's Daqin heavy-haul railway.

Item	Distances	Braking time	Release time	Y/Q	Wheelset lateral force (kN)	Middle coupler force (kN)	Rear coupler force (kN)	Coupler yaw angle (°)
1	K63 + 164	12:31:18	12:33:01	0.27	31	−1257	−1337	2.1
2	K141 + 108	13:34:32	13:37:37	0.23	28.6	−771	−871	1.7
3	K158 + 731	13:54:02	13:56:23	0.17	28	**−1450**	**−1539**	1.4
4	K176 + 260	14:10:26	14:14:09	0.22	15.6	−1195	−1240	1.5
5	K278 + 503	15:33:44	15:37:08	0.21	31.4	−1060	−1070	2
6	K290 + 229	15:46:56	15:53:04	**0.45**	**35**	−1122	−1206	**3.7**
7	K310 + 822	16:08:39	16:17:24	0.37	29	−478	−668	2.5

Note: Bold values represent the maximum in the columns.

railway. As shown, the coupler's longitudinal forces on the middle locomotives are more than 1000 kN at the long down ramp near the distance of K63. In the two cycle braking test sections, the coupler longitudinal forces in the interval of K141–K181 are larger than in the interval of K275–K325, but the lateral forces of the coupler and the wheelset in the interval of K275–K325 are larger.

Contrasting the simulation results, the AAR4 class irregularity is adopted to simulate the section of K275–K325 and the AAR5 is suitable for the section of K141–K181. In the several tests, the couplers were stable and the maximum yaw angle of the coupler reached 3.7°. The simulation results of the maximum yaw angle of the coupler are closer to the line test results and proved the accuracy of the coupler's dynamic model.

7. Conclusions

(1) This type of coupler exhibits self-stabilisation at a small yaw angle. The yaw angle of force line is less than the coupler's actual yaw angle, which helps to reduce the coupler lateral force. The small yaw resistance of the coupler because of the rolling friction of the contact surfaces is conducive to reduce the coupling of the two car bodies.

(2) The coupler's lateral forces are balanced by the secondary suspension of the locomotive. When the yaw moment of the coupler is greater than the anti-moment of the secondary suspension, the locomotive will be derailed. Increasing the secondary lateral stiffness and the friction coefficient of arc surfaces as well as reducing the secondary lateral stopper clearance are conducive to improve the bearing capacity of this type of coupler.

(3) The friction coefficient of the arc contact surface needs to be increased as the longitudinal compressive force of the coupler increases. The locomotive's coupler stability had been improved significantly by improving the parameters of the secondary structure. When the maximum coupler longitudinal compressive force reaches 2500 kN, the required friction coefficient is reduced from 0.6 to 0.35 relative to the original locomotive. This reduces the locomotive's derailment risks.

(4) The critical instability angles of the coupler are mainly related to the friction coefficient of arc contact surfaces. When the friction coefficient is 0.3, the critical instability angle is 4.0–4.5°. When the friction coefficient is 0.4, the critical instability angle is 4.5–5.5°.

Acknowledgements

The authors wish to acknowledge the support of the National Natural Science Foundation of China (No. 51205324), the Basic Application Research Foundation of Sichuan (No. 2012JY0021) and Independent Research and Development Project of Key Laboratory (No. 2011TPL_T04).

References

[1] Pugi L, Rindi A, Ercole AG, Palazzolo A, Auciello J, Fioravanti D, Ignesti M. Preliminary studies concerning the application of different braking arrangements on Italian freight trains. Veh Syst Dyn. 2011;49:1339–1365.
[2] Ma W, Luo SH, Song RR. Coupler dynamic performance analysis of heavy haul locomotive. Veh Syst Dyn. 2012;50:1435–1452.
[3] Noughabi SM. Dehghani K. Failure analysis of automatic coupler SA-3 in railway carriages. Eng Fail Anal. 2007;14:903–912.
[4] Railway Investigation Report R02C0050. Derailment, Canadian National Train NumberA-442-51-08 Mile 52.1, Transportation Safety Board of Canada, Camrose Subdivision Near Camrose, Alberta, 8 July; 2002.
[5] Belforte P, Cheli F, Diana G. Numerical and experimental approach for the evaluation of severe longitudinal dynamics of heavy freight trains. Veh Syst Dyn. 2008;46:937–955.
[6] Yao Y, Zhang HJ, Li YM. The dynamics study of locomotive under saturated adhesion. Veh Syst Dyn. 2011;49(8):1321–1338.
[7] Geike T. Understanding high coupler forces at metro vehicles. Veh Syst Dyn. 2007;45:389–396.
[8] Cole C, Mitchell M, Dudley R, Gerhard L, Fanus W, Ted M. Heavy haul coal train dynamics simulation comparisons of the COALlink and central Queensland systems. Proceedings of the 7th international heavy haul conference; 2001; Brisbane, Australia; p. 217–223.
[9] Simson SA, Cole C. Simulation of curving at low speed under high traction for passive steering hauling locomotives. Veh Syst Dyn. 2008;46:1107–1121.
[10] Cole C, Sun YQ. Simulated comparisons of wagon coupler systems in heavy haul trains. Proc IMechE F: J Rail Rapid Transit. 2006;220:247–256.
[11] Durali M, Shadmehri B. Nonlinear analysis of train derailment in severe braking. J Dyn Syst Meas Control, ASME. 2003;125:48–53.
[12] Geike T. Understanding high coupler forces at metro vehicles. Veh Syst Dyn. 2007;45:389–396.
[13] Pugi L, Fioravanti D, Rindi A. Modeling the Longitudinal Dynamics of Long Freight Trains During the Braking Phase. 12th IFTOMMWorld Congress; 2007 June; Besancon; p. 1–6.
[14] Wu Q, Yang XJ, Luo SH. Simulated study of the coupler/draft gear system for type HXD1 heavy haul locomotive. Electric Locomot Mass Transit Veh. 2013;35:25–28 (in Chinese).
[15] Zhai WM. Vehicle–track coupling cynamics. 3rd ed. Beijing: Science Press, Beijing; 2007 ISBN 978-7-03-018326-2 (in Chinese).